Chemical design of self-propelled Janus droplets

Caleb H. Meredith[1], Alexander Castonguay[2], Yu-Jen Chiu[1], Allan M. Brooks[3], Pepijn Moerman[4], Peter Torab[5], Pak Kin Wong[5,6,7], Ayusman Sen[2,3], Darrell Velegol[3], Lauren D. Zarzar[1,2,8*]

1. Department of Materials Science and Engineering, The Pennsylvania State University, University Park, PA 16802, USA
2. Department of Chemistry, The Pennsylvania State University, University Park, PA 16802, USA
3. Department of Chemical Engineering, The Pennsylvania State University, University Park, PA 16802, USA
4. Department of Chemical and Biomolecular Engineering, Johns Hopkins University, Baltimore, MD 21218, USA
5. Department of Mechanical Engineering, The Pennsylvania State University, University Park, PA 16802, USA
6. Department of Biomedical Engineering, The Pennsylvania State University, University Park, PA 16802, USA
7. Department of Surgery, College of Medicine, The Pennsylvania State University, Hershey, PA 17033, USA
8. Materials Research Institute, The Pennsylvania State University, University Park, PA 16802, USA

*Correspondence to ldz4@psu.edu

Significance Statement

Active materials capable of autonomous movement are of interest for understanding and harnessing the emergent properties of out-of-equilibrium systems. Multiphase fluids, such as emulsions, are an exciting platform for producing increasingly complex active colloids given their liquid-liquid interfaces which enable dynamic control over chemical transport and partitioning between fluid compartments. Here, we investigate the active behavior and underlying chemomechanical mechanisms imparting motility to microscale, self-propelled, solubilizing Janus oil droplets. A key discovery is that the two compartments of the biphasic Janus droplets function cooperatively via oil partitioning to govern droplet speed, direction, and propulsion efficiency.

Abstract

The study of active colloidal microswimmers with tunable phoretic and self-organizational behaviors is important for understanding out-of-equilibrium systems and the design of functional, adaptive matter. Solubilizing, self-propelling droplets have emerged as a rich chemical platform for exploration of active behaviors, but isotropic droplets rely on spontaneous symmetry breaking to sustain motion. The introduction of permanent asymmetry, e.g. in the form of a biphasic Janus droplet, has not been explored previously as a comprehensive design strategy for active droplets, despite the widespread use of Janus structures in motile solid particles. Here, we uncover the chemomechanical framework underlying the self-propulsion of active, biphasic Janus oil droplets solubilizing in aqueous surfactant. We elucidate how droplet propulsion is influenced by the degree of oil mixing, droplet shape, and oil solubilization rates for a range of oil combinations. A key finding is that for droplets containing both a mobile (solubilizing) and non-mobile oil, the degree of partitioning of the mobile oil across the Janus droplets' oil-oil interface plays a pivotal role in determining the droplet speed and swimming direction. As a result, we observe propulsion speeds of Janus droplets more than an order-of-magnitude faster than chasing pairs of single emulsion droplets which lack an oil-oil interface. In addition, spatiotemporal control over droplet swimming speed and orientation is demonstrated through the application of local thermal

gradients applied via induced via joule heading and laser spot illumination. We also explore the interactions between collections of Janus droplets including the spontaneous formation of multi-droplet spinning clusters that rotate predictably based on symmetry. Our findings provide key insights as to how the chemistry and structure of multiphase fluids can be harnessed to design microswimmers with programmable active and collective behaviors.

Introduction:

Active, colloidal microswimmers of diverse compositions and propulsion mechanisms are of interest as minimal models to probe out-of-equilibrium behavior and collective organization. For a colloid to exhibit self-propulsion, asymmetric forces must be continually present. A common microswimmer design strategy is to create solid colloids with permanent geometric or chemical asymmetry, i.e. Janus particles[1,2]. Localized chemical reactions occurring at the particle surface lead to gradient distributions of products that cause particle propulsion by mechanisms such as self-electrophoresis[3], self-diffusiophoresis[4,5], or bubble release[6]. Isotropic liquid droplets can also self-propel via the Marangoni effect, but local chemical gradients must be maintained by a hydrodynamic instability[7,8] or be externally applied[9]. Liquid Janus droplets, wherein the droplet is composed of two immiscible fluids each having an interface with the continuous phase, have been widely explored for uses such as particle templates[10,11], optics[12,13], and sensors[14,15], but few examples of self-propelled Janus droplets have been described[16-18]. However, Janus droplets present exciting opportunities for control of chemotactic colloidal interactions, given the presence of multiple fluid phases that enable dynamic changes in chemical partitioning, and the tunability of droplet morphology via modification of droplet and surfactant chemistry. Here, we explore systematically how chemical composition, oil partitioning, droplet shape, and solubilization cooperatively influence the propulsion of Janus oil droplets in aqueous surfactant. By providing a deeper understanding of the principles and trends influencing Janus droplet swimming behaviors, we aim to demonstrate that such droplets can serve as a robust material platform for rational design of chemically-responsive, self-propulsive colloids.

The simplest droplet swimmers consist of a single dispersed fluid phase within a continuous phase, such as spherical oil droplets in water[19,20] or water droplets in oil[21]. Active behavior is typically generated either by a reaction occurring at the droplet interface[22] or by droplet solubilization into surfactant micelles[23] that creates interfacial tension gradients and propels the drops via the Marangoni effect[24]. In the case of solubilization-driven propulsion, higher concentrations of solubilizate- "filled" micelles have been associated with higher interfacial tensions, causing droplets to move towards regions of solution containing more "empty" micelles and minimize interfacial energy[25]. Droplets can become self-propelled due to repulsion from their own solubilizate gradient when hydrodynamic instabilities result in spontaneous symmetry breaking of the fluid flows surrounding the droplet[21,26]. Overlap of chemical gradients resultant from nearby solubilizing droplets[20,27,28] , externally applied chemical gradients[9,19], internal droplet asymmetries[29], and interfacially adsorbed particles[30] are also possible sources of chemical asymmetry that can induce droplet motion. Recently, we described how oil droplets exhibit predator-prey chasing interactions when placed in a system containing at least two droplet "species" of different chemical composition that act together in a source-sink framework[31]. A solubilizing predator droplet acts as an oil-filled micelle source, while nearby prey droplets uptake the predator's oil, acting as a sink. The prey's attenuation of the oil concentration attracts the predator drops while the prey drops are repulsed by the approaching predator, resulting in a chase. Inspired by the synergy resultant from the dynamic exchange of oils with different solubilization profiles and chemistry, and the inherent asymmetry that can be attained in a Janus colloid structure[1], we sought to investigate the active behavior of solubilizing, biphasic Janus droplets.

In this work, we examine how the active swimming behaviors of Janus, biphasic oil-in-water droplets in surfactant are affected by droplet shape, droplet-internal oil partitioning, and oil solubilization

kinetics. By characterizing Janus droplets containing many different combinations of oils in Triton X-100 surfactant, we elucidate the relationships between the degree of oil mixing, interfacial tensions, and oil solubilization rates and their effects on droplet propulsion. A key conclusion is that for droplets containing both a mobile (solubilizing) and non-mobile oil, the degree of partitioning of the mobile oil across the Janus droplets' oil-oil interface critically influences droplet speed and swimming direction. As a result, the propulsion speeds of Janus droplets containing an oil-oil interface can be over an order-of-magnitude faster compared to chasing pairs of single emulsion droplets of the same chemical composition and size. Tuning of the Janus droplet compartment volume ratios, surfactant concentration, and solution temperature allow further control over the Janus droplet propulsion. Spatiotemporal control over the swimming speed and orientation of droplets is demonstrated by applying thermal gradients induced via joule heating and laser spot illumination. We also explore interactions between Janus droplets, including the spontaneous formation of multi-droplet spinning clusters that rotate predictably based on cluster symmetry. Our findings provide insight as to how the chemistry and structure of multiphase droplets can be harnessed to design microswimmers with programmable self-propulsive and collective behaviors.

Results and Discussion

Comparison of chasing single emulsion droplets and Janus droplets. To investigate swimming Janus droplet behavior, we began by exploring Janus droplets containing a pair of oils that already are known to exhibit chasing behavior[31] when present together as separate single emulsion droplets: 1-iododecane and ethoxynonafluorobutane (EFB) with drop diameters of approximately 60 µm in 0.5 wt% Triton X-100 (Triton) nonionic surfactant (**Figure 1a**). Both oils sink in the aqueous solution lending to ease of experimentation. Iododecane predator droplets readily undergo micellar solubilization (droplet diameter decreases by 0.22 µm/min) while EFB prey droplets have negligible solubilization. Once iododecane catches the EFB, the droplets form a pair that translates at speeds of up to 13 µm/s via the source-sink oil exchange framework previously described[31] (**Figure 1ai**). We prepared stable Janus droplets of iododecane and EFB in 0.5 wt% Triton using flow-focusing microfluidics, which allowed us to control the size of the droplets and the volume ratio of oils (**Figure 1aii**, **Figure S1**). The resultant shape of the droplets is governed by the balance of interfacial tensions[32,33].

We found that the iododecane-EFB Janus droplets dispersed in 0.5 wt% Triton swam in the same directional manner as the chasing droplet pair (i.e. iododecane in back, EFB in the front) but moved at speeds more than an order of magnitude faster, about 200 µm/s with long persistence lengths, many times the droplet length (**Figure 1aii, Video S1**). The Janus droplet speed gradually decreased over the droplet lifetime, which could be over an hour, as the iododecane tail of the droplet shrank and eventually disappeared due to solubilization (**Figure 1b**). Based on the observed droplet speeds and rate of volume change, the propulsion efficiency of the Janus droplet swimmer is estimated to be approximately 14 times greater than the chasing single emulsion droplets of the same chemistry and size (see Supporting Information, "Propulsion efficiency comparison"). Higher surfactant concentrations correlated to faster swimming (**Figure 1c**). No droplet motion was observed at Triton concentrations below the critical micelle concentration (CMC) or when surfactant solution was pre-saturated with both oils, indicating that the droplet swimming mechanism depended on the kinetics of micelle-mediated oil solubilization. When a second, fluorinated surfactant that solubilized the EFB was added, 1 wt% Capstone FS-30, no droplet motion was observed. Thus, preferential solubilization of one of the oils appeared important to the propulsion. The ratio of the Janus droplet compartment size (**Figure S2a,b**) and overall droplet size (**Figure S2c**) did influence the speeds, but all of these Janus droplets examined were still much faster than the chasing single emulsion droplet pair.

As such, it appeared that the mere presence of the oil-oil interface was also a critical contributor to Janus drop swimming. An oil-oil interface would be expected to enable the direct partitioning of the oils between the Janus droplet compartments, whereas micelle-mediated oil transfer through the water

is required for chasing single emulsion droplets to exchange oil. These different pathways for oil transport, we suspected, could be largely influential over the droplet swimming dynamics and required further investigation.

Influence of chemical composition and oil partitioning on Janus droplet propulsion speed and direction. To explore the influence of chemical partitioning across the oil-oil interface on the Janus droplet propulsion, we systematically varied the oil compositions and examined trends in droplet speed and shape (**Figure 2**). We note that when changing oil compositions, we are altering more than just chemical partitioning; the droplet shape can change due to alterations in the balance of interfacial tensions[32,33], and oil solubilization rates[34] – which provide the fuel for propulsion – can change as well. We attempt to consider these factors when designing the experiments and interpreting the results as described below.

We first examined Janus droplets containing iododecane paired with several other fluorinated oils of varying degrees of fluorination: methoxyperfluorobutane (MFB), 2-(trifluoromethyl)-3-ethoxydodecafluorohexane (HFE-7500), perfluorohexane (PFH), perfluorooctane (PFO) and perfluorotributylamine (FC-43) (**Figure 2**). None of these fluorinated oils solubilize to a measurable extent in 0.5 wt% Triton, and they have, respectively, a decreasing degree of partitioning into iododecane at room temperature as measured by changes in refractive index (**Figure S3**, Methods "Oil partitioning measurement"). We presume that the same partitioning trends also hold when considering the amount of iododecane in the fluorinated oil. All the fluorinated oil pairings with iododecane produced stable Janus droplets with similar shapes, and all the Janus droplets swam in the same direction, with the solubilizing iododecane oil in the back (**Figure 2a, yellow**). However, the droplets swam at very different speeds depending on the non-solubilizing fluorinated oil; the smaller the degree of oil partitioning, the slower the speed. For instance, iododecane-EFB droplets swam at 196 ± 4 μm/s and had 7.9 vol% of EFB in iododecane, whereas iododecane-FC-43 droplets swam at 12 ± 2 μm/s with <0.1 vol% partitioning.

When iododecane was replaced with the shorter chain length iodononane, droplet speeds increased overall (**Figure 2a, orange**), while replacement with longer chain length iodododecane led to reduced speeds (**Figure 2a, blue**). Most of the droplets had similar shapes. Partitioning of the fluorinated oils with the iodononane and iododecane were similar to the iododecane (10.0 vol% vs. 7.9 vol%) (**Figure S3a**). However, the solubilization rate of iodononane was much faster (0.34 ± 0.03 μm/min) and iodododecane much slower (0.09 ± 0.01 μm/min) than the iododecane (0.22 ± 0.02 μm/min) (**Figure S4a**). Thus, we conclude that when controlling for droplet shape and degree of partitioning, faster micelle-mediated solubilization led to faster Janus droplet swimming.

When we changed the halogen atom on the haloalkane oil while maintaining carbon number (e.g. 1-chloro-, 1-bromo-, and 1-iododecane), we saw a greater diversity of droplet morphologies and a wider range of degrees of partitioning which corresponded to greater variation in the Janus droplet speeds (**Figure 2b, Figure S3b**). We take chlorodecane as the example to discuss the observed effects of droplet shape on the speed (**Figure 2b, grey**). Chlorodecane and EFB are fully miscible, forming a single emulsion droplet that did not swim. Chlorodecane paired with MFB or HFE-7500 remained phase-separated but formed double or near-double emulsion droplets that swam slowly, if at all (<5 μm/s). The degree of partitioning in these two aforementioned oil pairs (13.6 vol% and 7.4 vol% respectively) is on par with that of iodononane paired with EFB or MFB (5.7 - 10.0 vol%) and chlorodecane also solubilizes at a similar rate to iodononane (0.41 μm/min vs. 0.34 μm/min). However, dumbbell-shaped iodononane-EFB and iodononane-MFB Janus droplets swam an order of magnitude faster than the more encapsulated chlorodecane-MFB and chlorodecane-HFE-7500 drops, suggesting that the droplet shape asymmetry plays a significant role in droplet speed. Chlorodecane paired with PFH and PFO formed more dumbbell-like droplets and, correspondingly, swam significantly faster (159 and 145 μm/s). Chlorodecane paired with FC-43 formed a near-double emulsion drop shape and again swam more slowly (43 μm/s) and with shorter persistence lengths on the order of the droplet length, having both an unfavorable encapsulated

drop shape as well as low degree of oil partitioning (≈0.1 vol%). Thus, we conclude that an anisotropic Janus droplet shape contributes to faster propulsion.

For all oil combinations in **Figure 2**, the Janus droplets swam with the mobile, solubilizing haloalkane in the back and the non-mobile fluorinated oil in the front. However, when we examined Janus droplets containing a non-mobile fluorinated silicone polymer (25%-35% nonafluorohexylmethylsiloxane, 65-75% dimethyl siloxane copolymer, 8-12 cP) paired with mobile dibromooctane (solubilization rate = 0.65 μm/min), we noticed anomalous behavior; upon adding these droplets to fresh 0.5 wt% Triton, they initially propelled with the dibromooctane in back at speeds of more than 60 μm/s, but after tens of seconds, slowed to a halt then swam in the reverse orientation at peak speeds of only about 13 μm/s (**Video S2**, **Figure 3a**). The droplets remained swimming in this 'reverse' orientation until all the dibromooctane had been solubilized. Reversal in the swimming orientation was also observed for dibromooctane paired with 100 cP and 10,000 cP polydimethylsiloxane. The reversal in swimming orientation suggests that the oil solubilization profile of the droplets changes a function of time to reach a different steady state condition than the 'forward' swimmers. Since the non-mobile oil compartment in the reverse swimmers is higher viscosity than the forward swimmers, potentially, the mobile oil is not able to continuously repartition fast enough during droplet swimming to maintain a critical steady state concentration of mobile oil and solubilization rate on both sides of the droplet necessary for forward motion. Variation in the concentration profiles of oil-filled micelles across the droplets surface could lead to differences in the interfacial tension gradients across the droplet surface and different propulsion direction.

To compare the forward and reverse orientation swimmers, we used particle image velocimetry (PIV) to map the external flows (**Figure 3b**, **Video S3**). Results revealed distinct Marangoni force-generated flow profiles that suggest differences between the swimming mechanisms. The majority of the flow in the plane of movement surrounding the forward Janus swimmer were emitted opposite the direction of motion. The reverse swimmer, however, had its fastest flows in the directions perpendicular to droplet motion which do not contribute towards propulsion and also carried a small eddy of flow at the rear of the droplet. In both swimming cases, the planar flow field we measure shows a net flow extending from the droplet, indicating a possible contribution of non-visualized fluid from the direction above the droplets as they move.

Proposed Janus droplet swimming mechanism as influenced by oil partitioning, droplet shape, and solubilization rates. Based on the observed correlations between droplet shape, solubilization rates, oil partitioning, and droplet speed described in **Figures 1-3**, we propose the following generalized framework for rationalizing Janus droplet swimming behaviors (**Figure 4**). Janus droplet motion is driven by Marangoni flows resultant from an asymmetric distribution of a mobile (solubilizing) oil across the droplet surface. Higher concentrations of solubilized oil correspond to higher interfacial tensions resultant from oil-surfactant interactions[25]. To minimize surface energy, droplets propel towards regions with lower concentrations of solubilized oil and more "free" surfactant. While this general propulsion mechanism is similar to that of solubilizing single emulsion droplets, there are several additional considerations for swimming Janus droplets.

In a Janus droplet, there are two oils present; these two oils can be either both mobile, both non-mobile, or one mobile and one non-mobile. If both oils are non-mobile, the droplet will not swim via a solubilization-driven mechanism, so we do not consider this case further. The oils can also have different degrees of partitioning within each other, governing the concentrations of each oil within each compartment of the Janus droplet; we expect this to affect the rate of solubilization of the mobile oil across each compartment's interface. Further, the oils can assume different geometries within the droplet as governed by the balance of interfacial tensions[32,33]. The droplet shape affects the gradient profile of the oil released by solubilization. We conceptually consider each of these combinations of factors below

in four general cases, depicted in **Figure 4**. We note that these four cases are simplified and meant to provide principles to guide the design of active Janus droplets with control over speed, persistence, and directionality. Future work, including development of fluid mechanical models, would be necessary to fully understand how the droplet shapes, solubilization kinetics, interfacial tension gradients, and non-equilibrium oil partitioning balance to govern the Janus droplet swimming dynamics.

Case 1. A nearly encapsulated Janus droplet (or double emulsion) containing at least one solubilizing oil. For a droplet in which one oil is fully or near fully encapsulated by the other, the gradient of solubilized oil is largely symmetric. This case is more comparable to a self-propelled single emulsion droplet having high symmetry such that spontaneous symmetry breaking and hydrodynamic instabilities are necessary to maintain motion. This case is exemplified by chlorodecane-MFB, chlorodecane-HFE-7500, bromodecane-EFB or chlorodecane-FC-43 droplets in **Figure 2**.

Case 2. An anisotropic Janus droplet containing mobile and non-mobile oil compartments with negligible partitioning. In this case, the mobile oil solubilizes nearly exclusively from only one compartment of the Janus droplet, and the droplet will propel with the mobile oil compartment in the front, non-mobile oil compartment in the back, in order to maximize the advection of surfactant solution containing more empty micelles to the droplet interface. This case is exemplified by the dibromooctane-fluorosilicone droplets in Triton, wherein we propose that the reversal in droplet orientation is due to the fact that the mobile dibromooctane cannot continually repartition into the fluorosilicone as quickly as it is solubilized from the fluorosilicone during swimming; this leads to the eventual depletion of the mobile oil within the non-mobile oil compartment and the swimming direction reversal. This case also likely describes the swimming of Janus droplets containing non-solubilizing silicone polymer and solubilizing liquid crystal oils as reported in the literature[17].

Case 3. An anisotropic Janus droplet containing mobile and non-mobile oils with some degree of oil partitioning. The mobile oil having finite solubility in the non-mobile oil compartment can partition across the oil-oil interface and therefore solubilize along the entire surface of the Janus droplet. Since the mobile oil is present in different concentrations within the drop compartments, we expect that the mobile oil may solubilize at different rates from each compartment[34]. An extended, anisotropic gradient of solubilized oil across the length of the entire droplet is generated. As the droplet swims, the mobile oil redistributes across the oil-oil interface to maintain a steady state concentration and continuous solubilization across the length of the droplet. The majority of the droplets in **Figure 1** and **Figure 2** exemplify this situation.

Case 4. An anisotropic Janus droplet with similar micelle-mediated solubilization from both compartments. If micelle-mediated solubilization is occurring uniformly around the entire Janus droplet, the interfacial tension gradients will be minimized and so the droplet may move slowly or not move at all. We observed this case for a Janus droplet containing two mobile oils: iododecane-EFB droplets in a surfactant mixture of Capstone FS-30 and Triton. We imagine that this case could also occur if the mobile oil partitioning into the non-mobile oil was very high such that the mobile oil was solubilizing at similar rates across the entire droplet surface resulting in a symmetrical distribution of oil-filled micelles.

Harnessing thermal gradients to manipulate Janus droplet dynamics. Following from our proposed framework, we expect that application of stimuli which modify oil partitioning, solubilization rates, and droplet shapes can be used to manipulate Janus droplet swimming behaviors. Higher temperatures, for instance, are expected to accelerate the kinetics of oil solubilization[34] as well as favor mixing between the haloalkanes and fluorinated oils[35]. To examine how temperature would affect droplet swimming, we used a temperature regulated microscope chamber and measured the swimming speed of iododecane-EFB Janus drops in 0.5 wt% Triton between 10 °C and 50 °C. As the temperature was increased from 10 °C to 30 °C, Janus droplet speed steadily increased, as did the iododecane solubilization rate as evidenced by faster shrinkage of the droplet volume (**Figure 5a**). However, at temperatures above 30 °C,

the Janus droplet shape changed, and the droplet speed slowed, even though iododecane was still solubilizing. We attribute this speed reduction to the more spherical droplet shape (i.e. "Case 1"); it is also possible that the iododecane may be solubilizing at similar rates from both sides of the Janus droplet due to higher partitioning at these elevated temperatures (i.e. "Case 4") thereby reducing the asymmetry in the oil gradient, although this is difficult to experimentally probe. By substituting EFB with HFE-7500, a more highly fluorinated oil that has less favorable mixing with the iododecane, the maximum swimming speed could be raised above 420 μm/sec at temperatures between 40 °C and 50 °C, and the droplets did not become more spherical at higher temperatures.

To examine the effect of thermal gradients as a possible method to control droplet swimming behavior, we used a microscale Joule heater under different applied voltages (**Figure S5**) and used an IR camera to map the thermal profile as a function of distance from the electrodes (**Figure 5b,** bottom plot). Droplets of iododecane-EFB droplets in 0.5 wt% Triton with 0.1 M NaCl were added 10 mm away from the heater and their positions with corresponding speeds were analyzed (**Figure 5b**, top plot). Under the application of a voltage, droplets swam towards the heater electrodes and accelerated as they approached, directionally propelling up the thermal gradient even when the gradient was minimal, <0.5 °C/mm. Control experiments conducted with 75-90 μm polyethylene tracer particles (1.02 g/cm^3) and single emulsion droplets composed of either iododecane and EFB oils produced significantly reduced motion (<20 μm/s within 500 μm of heater under the highest voltage) , ruling out effects of heating-driven convection and thermocapillary motion as primary causes of the observed acceleration of Janus droplets as they approached the heater.

After establishing that thermal gradients are effective stimuli for control of droplet speed and orientation, we sought to manipulate the Janus droplets with a more easily patternable heat source: a continuous wave near-infrared laser (780 nm) focused through the bottom of the sample chamber. When the laser was focused in a fixed position, randomly swimming iododecane-EFB Janus droplets in 0.5 wt% Triton gathered around the laser spot over the course of a few minutes in a radial fashion with the EFB compartment closer to the laser (**Figure 5c, Video S4**)**.** As the size of the assembled droplet cluster grew, an area depleted of droplets surrounding the laser beam began to form (**Figure 5c,** rightmost panel). We attribute this depletion zone to convective flows which draw oil-saturated surfactant solution along the dish bottom towards the center of the droplet cluster, imparting a repulsive force that balances the attraction of droplets towards the higher temperature center. By scanning the laser beam across collections of droplets, we could direct the droplet orientation, although the orientation remained stable only for several minutes after the beam had passed (**Figure 5d, Video S5**).

Janus droplet interactions and collective behaviors. Solubilizing droplets not only respond to self-generated gradients, but they can also respond to the chemical gradients produced by droplet neighbors, leading to multibody and collective interactions[27,36]. As shown previously in **Figure 1**, isolated Janus droplets of iododecane-EFB in 0.5 wt% Triton swam in a linear fashion with a stable speed of around 200 μm/s. However, when the number density of droplets was increased such that droplets were forced to swim through regions of solution recently occupied by another droplet, a slowdown in speed accompanied by a slight reorientation in direction often occurred (**Figure 6a,b, Video S6**). This slowdown is caused by the "exhaust trail"[37] of solubilized oil in micelles left behind as the droplets swim. As the chemical trail ages and oil-filled micelles diffuse, intersecting droplets experienced a smaller drop in speed as they crossed through the trail region (**Figure 6b,c**). We tracked and analyzed droplet speeds during more than 200 trail interaction events to generate a relative speed decrease vs. trail age dataset; when fitted to an exponential recovery model, this data gave a relaxation timescale in good agreement with the diffusivity of the Triton micelles[38] over the droplet trail width approximated using the Stokes-Einstein equation (**Figure 6c**, Supporting Information section "Analysis of droplet trail interactions").

Collective effects on active behavior due to multi-body droplet interactions were also observed when larger numbers of Janus droplets (hundreds to thousands) were added to the sample chamber leading to high local droplet number density. For example, Janus droplets of iododecane-MFB in 0.5 wt% Triton spontaneously formed coordinated clusters of three to five droplets which rotated at up to 28 revolutions per minute (rpm) (**Figure 6d**, **Video S7**). The rotating assemblies were stable for minutes and rotated in either clockwise or counter-clockwise directions dependent on the cluster symmetry. Reverse swimmers composed of dibromooctane-fluorosilicone in 0.5 wt% Triton also formed spinning clusters but the orientation of the Janus droplets within the spinner was flipped compared to the forward swimmers such that the solubilizing dibromooctane oil was closer to the cluster center (**Figure 6e**). Visualization of the external flows in the plane directly above spinning droplet assemblies using tracer particles revealed steady inward motion of fluid, while flows in the droplets plane were ejected outwards away from the cluster (**Figure 6f, Video S8**). These observations suggest that the formation of spinning assemblies may be favored due to a stable vortex of fresh surfactant solution being pumped downward by the cooperative rotating motion. If the Janus droplets were prevented from moving, such as by affixing iododecane-EFB Janus droplets to a glass coverslip by surface wetting, droplet pumps were generated that directionally moved fluid from the front of the droplet to the back (**Video S9**). Overall, control over the arrangement of droplets through their collective swimming interactions or the manipulation of thermal profiles may be used to spatially organize and harness the pumping behavior[39] of droplets.

Conclusions

We have shown that Janus oil droplets undergoing micellar solubilization in surfactant solutions can exhibit a rich diversity of controllable, active behaviors. Through a systematic investigation of oil chemistry and partitioning, droplet shape, surfactant conditions, and temperature, we have begun to elucidate the underlying drivers and key design principles that govern Janus droplet motion. Our experimental results point to the importance of oil partitioning between the Janus droplet compartments in determining droplet swimming speed and direction. We demonstrated many combinations of swimming Janus droplets containing haloalkane, fluorocarbon, and silicone oils, with speeds reaching over several hundred microns per second, and provide chemical design principles for tuning of the Janus droplet dynamics. Collective interactions between droplets, such as spinning droplet cluster formation and chemical trail interactions, were observed and analyzed. Further studies aimed at understanding and modeling the pathways and kinetics of solubilization in multiphase droplets will lead to additional insights for controlling droplet dynamics and multibody effects. We believe that active Janus droplets may be used to test and inspire new models for the collective dynamics of interacting microswimmers[40,41] and serve as the foundation for chemical design of more complex materials with emergent active behaviors[42-44].

Acknowledgments and funding

LZ acknowledges funding from the Army Research Office grant W911NF-18-1-0414 and the Marion Milligan Mason Award for Women in the Chemical Sciences. AS acknowledges funding by the Department of Energy, Office of Basic Energy Sciences (DOE-DE-SC0020964). PM acknowledges funding by Department of Energy Biomolecular Materials (DE-SC0010426)

Competing Interests. The authors declare no competing interests.

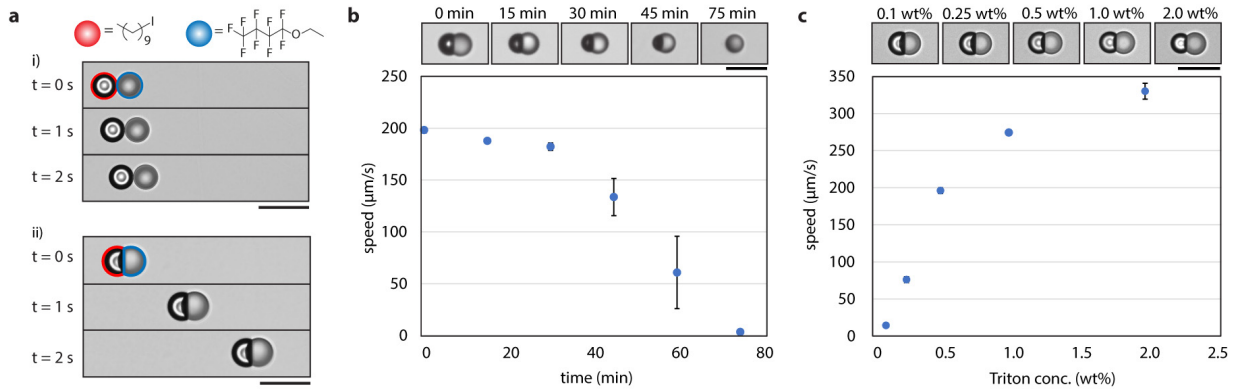

Figure 1: Iododecane and EFB oils paired in a Janus droplet exhibit faster speeds than chasing single emulsion droplets and speeds are dependent on oil compartment size and surfactant concentration.
a) Time sequence micrographs comparing: (i) the speed of chasing iododecane (red) and EFB (blue) single emulsion droplets, and (ii) a Janus droplet of the same oils in 0.5 wt% Triton. Scale, 100 µm. **b)** Janus droplets composed of iododecane and EFB oils in 0.5 wt% Triton show a gradual decline in speed over time as iododecane is solubilized. Optical micrographs of Janus droplets at varying timepoints are shown. Scale, 100 µm. **c)** The speeds of iododecane and EFB Janus droplets vary as a function of Triton surfactant concentration. Optical micrographs of Janus droplets at different Triton concentrations are shown. Scale, 100 µm.

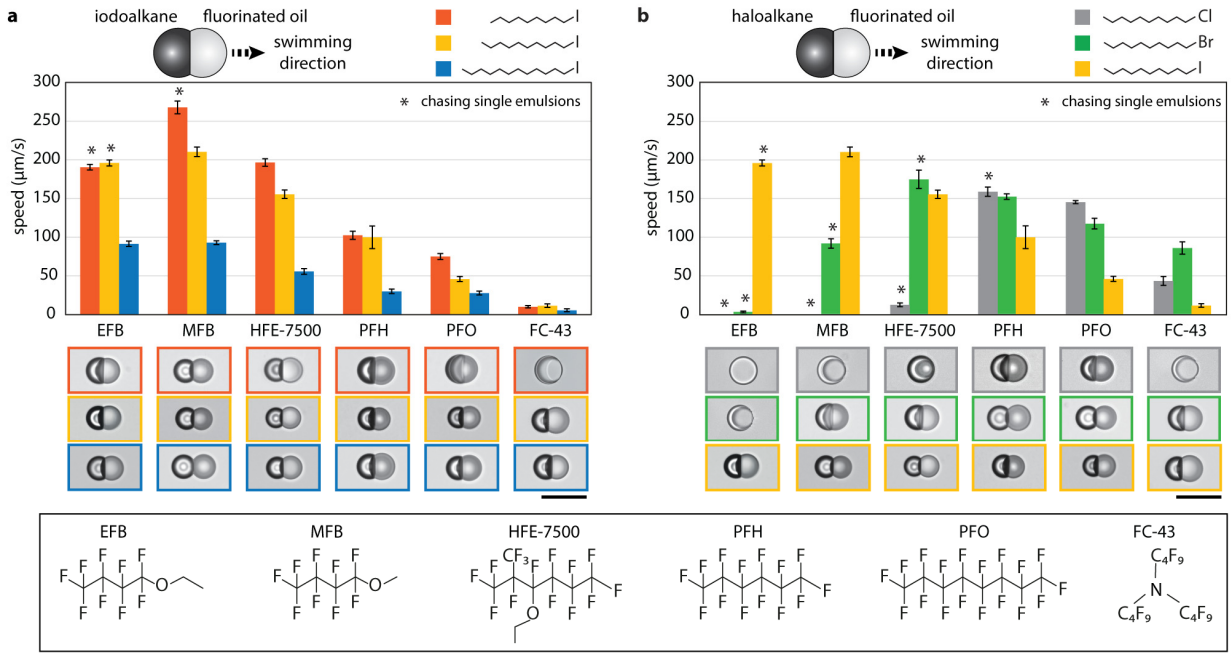

Figure 2: The partitioning of oils within the Janus droplet and the droplet shape influence the swimming speed. For both **(a)** and **(b)**, Janus droplets composed of varying haloalkane and fluorinated oils were made in 0.5 wt% Triton, and their speeds and droplet shapes were analyzed. In **(a)**, speeds of Janus droplets composed of iodoalkane oils of varying chain lengths each paired with several fluorinated oils were compared. In **(b)**, speeds of Janus droplets composed of 1-chloro-, 1-bromo, and 1-iododecane each paired with several fluorinated oils were compared. The ordering of the fluorinated oils along the x axis from left to right follows the trend of decreasing degree of partitioning of the haloalkane into the fluorinated oil (**Figure S3**). An asterisk (*) indicates oil pairings which exhibit single emulsion droplet chasing. Each data point represents the average value of five speed measurements obtained from the displacements of different droplets over a 5 second period with standard deviation error bars. Optical micrographs of the Janus droplets formed from each oil pairing are aligned beneath each plot. The colored border of the micrographs indicates the haloalkane, and the column indicates the fluorinated oil. The Janus droplet images are oriented with the haloalkane is the left-side compartment and the fluorinated oil is the right-side. If swimming, droplets move rightward. EFB and chlorodecane are miscible. Chemical structures of the fluorinated oils are given at bottom. Scale, 100 μm.

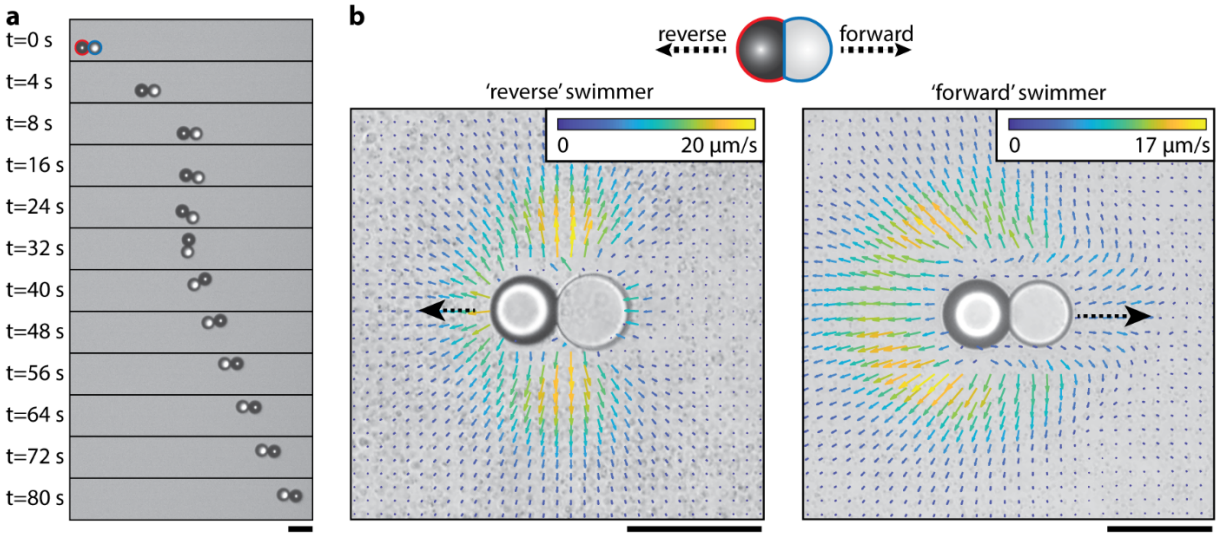

Figure 3: Janus droplet swimming orientation can reverse over time. a) Time sequence micrographs showing the swimming behavior of dibromooctane (red) and fluorosilicone (blue) Janus droplets in 0.5 wt% Triton. Initially, the droplet moves with dibromooctane in the back, fluorosilicone in the front (i.e. a 'forward' swimmer), but after a matter of seconds, the drop reverses orientation and moves with dibromooctane in front (i.e. 'reverse' swimmer). The droplet persists in this reverse orientation for the duration of its lifetime. See **Video S2**. Scale, 100 µm. **b)** The external flow profiles surrounding a Janus droplet composed of dibromorooctane fluorosilicone with 'forward' and 'reverse' swimming orientations in 0.5 wt% Triton solution visualized using PIV analysis of suspended tracer particles. See **Video S3.** Scale, 100 µm.

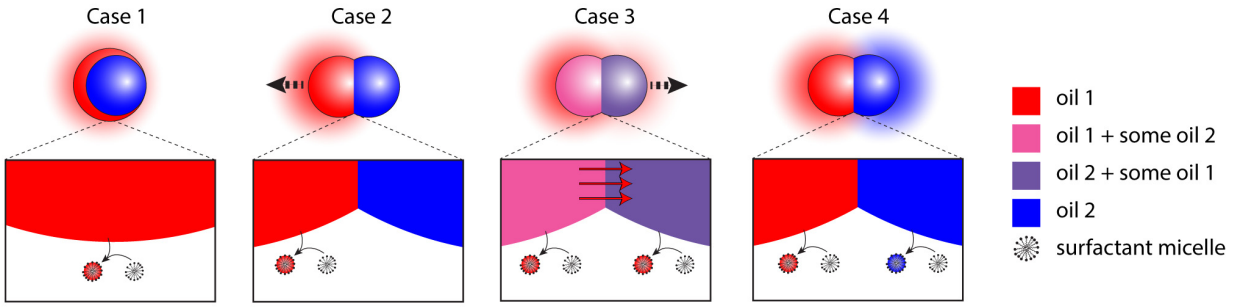

Figure 4: Balance between solubilization, oil partitioning across the Janus droplet's internal interface, and droplet shape affects swimming behaviors. Shown are schematics representing the swimming behaviors of four general droplet "cases" we have observed experimentally. Each droplet contains two oils (oil 1 and oil 2) in different geometries, with different degrees of mutual partitioning, and different micelle-mediated solubilization as depicted in the diagrams. **Case 1**: the droplet is quite spherical, e.g., a double or near-double emulsion, where oil 1 nearly fully encapsulates oil 2 and the solubilized oil gradient is largely symmetric. We find that such droplets tend to swim slowly, if at all. **Case 2**: an anisotropic Janus droplet is formed, but the mobile oil 1, is only solubilizing from one compartment. This case could arise because the oils do not partition into each other, or the rate of replenishment of oil 1 into the oil 2 compartment occurs slowly such that a significant steady-state concentration of oil 1 inside the oil compartment is not maintainable. We find that such droplets swim with the solubilizing oil in the front (i.e. the 'reverse' swimmers). **Case 3**: an anisotropic Janus droplet is formed, and the oils have mutual partitioning so as to maintain a swimming steady-state concentration of oil 1 inside the oil 2 compartment, and only oil 1 is solubilizing. The droplet swims with oil 1 in the back and oil 2 in the front (i.e. 'forward' swimmers). **Case 4**: an anisotropic Janus droplet is formed but both oil 1 and oil 2 can solubilize. We find these droplets to swim slowly, if at all.

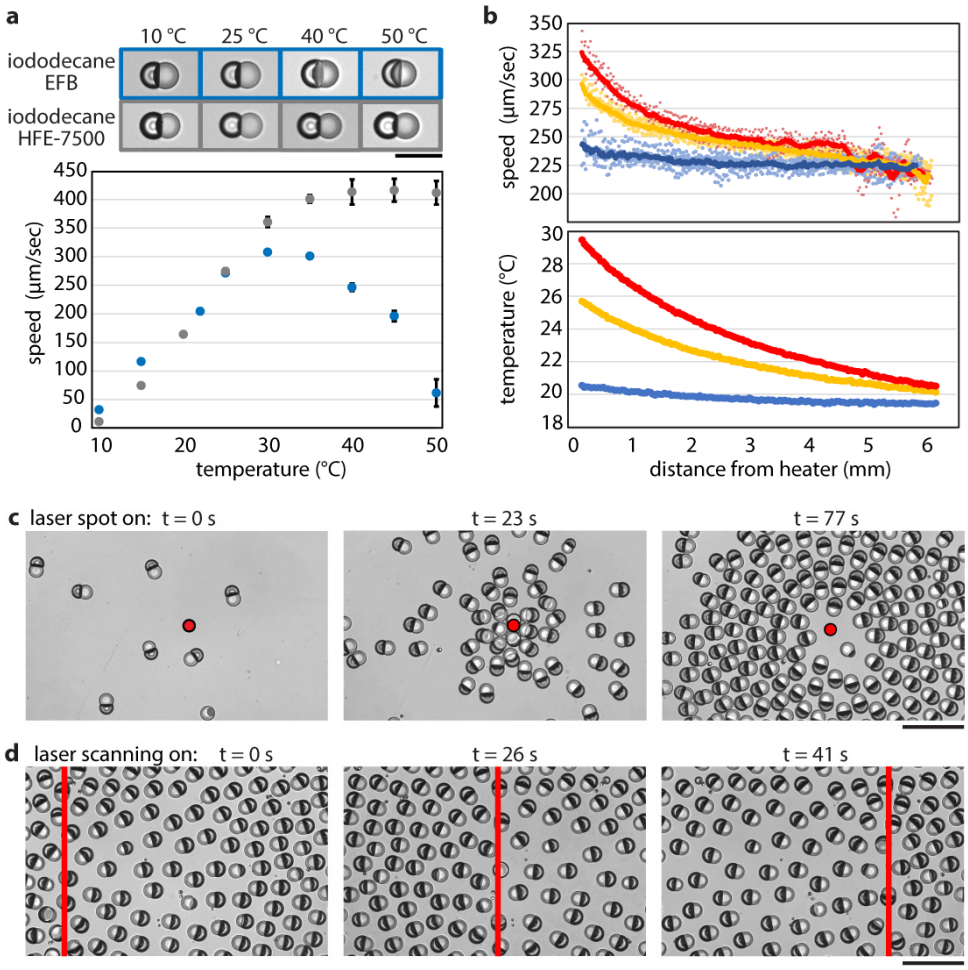

Figure 5: Thermal gradients are used to control Janus droplet speeds, positioning, and organization. a) The shapes and speeds of iododecane-EFB and iododecane-HFE-7500 Janus droplets in 0.5 wt% Triton were analyzed at temperatures between 10 °C and 50 °C. Each data point represents the average of five speed measurements obtained from the displacements of different droplets over a 5 second period with standard deviation error bars. Optical micrographs of droplets at different temperatures are given. Scale, 100 µm. **b)** A microscale Joule heater was used to apply a thermal gradient to iododecane-EFB droplets in 0.5 wt% Triton and 0.1 M NaCl solution. See **Figure S5** for a diagram of the heater design. Janus droplets were added 10 mm away from the heater electrodes and the droplet speeds were analyzed as a function of distance from the heater (top plot). Data points represent the instantaneous tracked speeds of five different droplets swimming towards the heater at each voltage, while the line represents the moving average determined by the nearest 10 data points. An IR camera was used to determine the solution temperature as a function of distance from the heater electrodes (bottom plot). **c)** Iododecane-EFB Janus droplets in 0.5 wt% Triton were exposed to a 780 nm laser at 250 mW, focused at the red dot in each optical micrograph. The laser was left "on" and over time the solution heated locally, attracting droplets that organized radially. The EFB side of the Janus droplet always pointed towards the laser. See **Video S4**. Scale, 250 µm. **d)** Iododecane-EFB Janus droplets in 0.5 wt% Triton were exposed to a scanning 780 nm laser. The laser was scanned back and forth along the red line at a rate of 0.2 pass/second. As the laser line was passed across the field of view, the droplets reoriented themselves such that the EFB side of the droplet always faced towards the laser. See **Video S5**. Scale, 250 µm.

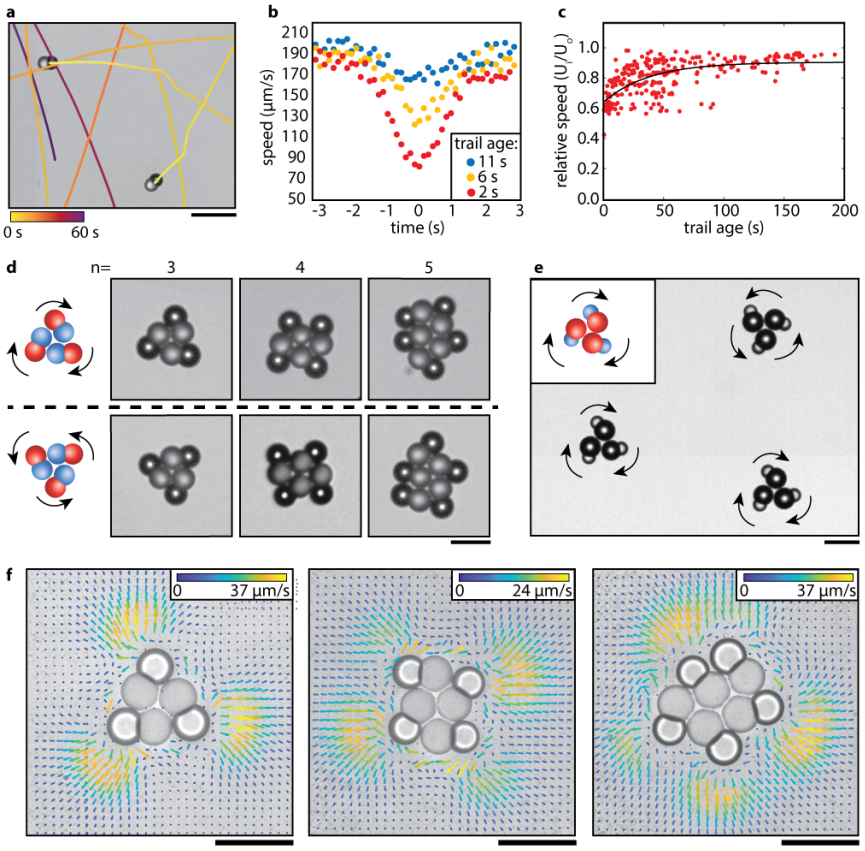

Figure 6: Multi-body interactions between Janus droplets. a) An optical micrograph shows iododecane-EFB Janus droplets in 0.5 wt% Triton with colored traces of the droplet trails over 60 seconds. Trails are color coded by lifetime according to the color scale. When droplets swim over a recent trail, they experienced a disturbance in their movement leading to a slight swerving of direction and slowdown in speed (**Video S6**). Scale, 250 μm. **b)** The speeds of individual iododecane-EFB Janus droplets were analyzed as they crossed over trails of solubilized oil left by other droplets while swimming in 0.5 wt% Triton. Data points represent the instantaneous speeds of three separate droplets while crossing over trails with ages of 2, 6, and 11 seconds. The timepoint of trail crossing was defined as zero seconds. **c)** The minimum speed of individual iododecane-EFB Janus droplets in 0.5 wt% Triton as they crossed a trail of solubilized oil were analyzed and plotted as a function of trail age. Speed values are presented as a relative fraction of the initial speed before and after the crossing event, obtained using a custom Matlab tracking tool. The black line represents the fitting of an exponential recovery model based on the scaling of the magnitude of speed decrease with the time lag between interactions. **d)** Assemblies of n=3, 4, or 5 Janus droplets composed of iododecane (red) and methoxyperfluorobutane (blue) in 0.5 wt% Triton spin directionally based on the assembly symmetry. Assemblies of n=3 rotate at 22 ± 5 rpm, n=4 rotate at 18 ± 4 rpm, and of n=5 rotate at 15 ± 3 rpm as determined from the average and standard deviation of five isolated droplet clusters measured over one minute. See **Video S7**. Scale, 100 μm. **e)** Reverse swimmers composed of dibromooctane (red) and fluorosilicone (blue) form assemblies that spin as well, but the solubilizing dibromooctane is at the cluster center. Arrows indicate spinning direction. Scale, 100 μm. **f)** External flow profiles surrounding spinning clusters of iododecane-methoxyperfluorobutane Janus drops in 0.5 wt% Triton obtained using PIV tracking of suspended tracer particles. Visualizing the external flows revealed the stability of droplet assemblies is sustained by a vortex of surfactant solution being pumped downward onto the cluster (**Video S8**). Scale, 100 μm.

References

1 Jurado-Sanchez, B., Pacheco, M., Maria-Hormigos, R. & Escarpa, A. Perspectives on Janus micromotors: Materials and applications. *Applied Materials Today* **9**, 407-418 (2017).

2 Paxton, W. F. *et al.* Catalytic nanomotors: autonomous movement of striped nanorods. *Journal of the American Chemical Society* **126**, 13424-13431 (2004).

3 Wong, F., Dey, K. K. & Sen, A. Synthetic micro/nanomotors and pumps: fabrication and applications. *Annual Review of Materials Research* **46**, 407-432, (2016).

4 Moran, J. L. & Posner, J. D. Phoretic self-propulsion. *Annual Review of Fluid Mechanics* **49**, 511-540 (2017).

5 Anderson, J. L. Colloid transport by interfacial forces. *Annual Review of Fluid Mechanics* **21**, 61-99 (1989).

6 Gao, W., Uygun, A. & Wang, J. Hydrogen-bubble-propelled zinc-based microrockets in strongly acidic media. *Journal of the American Chemical Society* **134**, 897-900 (2012).

7 Maass, C. C., Krüger, C., Herminghaus, S. & Bahr, C. Swimming droplets. *Annual Review of Condensed Matter Physics* **7**, 171-193, (2016).

8 Schmitt, M. & Stark, H. Swimming active droplet: A theoretical analysis. *EPL (Europhysics Letters)* **101**, 44008 (2013).

9 Lagzi, I., Soh, S., Wesson, P. J., Browne, K. P. & Grzybowski, B. A. Maze solving by chemotactic droplets. *Journal of the American Chemical Society* **132**, 1198-1199 (2010).

10 Lone, S. & Cheong, I. W. Fabrication of polymeric Janus particles by droplet microfluidics. *RSC Advances* **4**, 13322-13333 (2014).

11 Frank, B. D., Antonietti, M. & Zeininger, L. Structurally anisotropic janus particles with tunable amphiphilicity via polymerization of dynamic complex emulsions. *Macromolecules* (2020).

12 Goodling, A. E. *et al.* Colouration by total internal reflection and interference at microscale concave interfaces. *Nature* **566**, 523-527, (2019).

13 Nagelberg, S. *et al.* Reconfigurable and responsive droplet-based compound micro-lenses. *Nature Communications* **8** (2017).

14 Balaj, R. V. & Zarzar, L. D. Reconfigurable complex emulsions: Design, properties, and applications. *Chemical Physics Reviews* **1**, 011301 (2020).

15 Zarzar, L. D., Kalow, J. A., He, X., Walish, J. J. & Swager, T. M. Optical visualization and quantification of enzyme activity using dynamic droplet lenses. *Proceedings of the National Academy of Sciences* **114**, 3821-3825, (2017).

16 Li, M., Brinkmann, M., Pagonabarraga, I., Seemann, R. & Fleury, J.-B. Spatiotemporal control of cargo delivery performed by programmable self-propelled Janus droplets. *Communications Physics* **1**, 23, (2018).

17 Jeong, J. *et al.* Liquid crystal Janus emulsion droplets: preparation, tumbling, and swimming. *Soft Matter* **11**, 6747-6754 (2015).

18 Li, M. *et al.* Kinetics of active water/ethanol Janus droplets. *Soft Matter* **16**, 6803-6811 (2020).

19 Jin, C., Krüger, C. & Maass, C. C. Chemotaxis and autochemotaxis of self-propelling droplet swimmers. *Proceedings of the National Academy of Sciences* **114**, 5089-5094 (2017).

20 Moerman, P. G. *et al.* Solute-mediated interactions between active droplets. *Physical Review E* **96**, 032607 (2017).

21 Izri, Z., van der Linden, M. N., Michelin, S. & Dauchot, O. Self-propulsion of pure water droplets by spontaneous marangoni-stress-driven motion. *Physical Review Letters* **113**, 248302 (2014).

22 Hanczyc, M. M., Toyota, T., Ikegami, T., Packard, N. & Sugawara, T. Fatty acid chemistry at the oil− water interface: Self-propelled oil droplets. *Journal of the American Chemical Society* **129**, 9386-9391 (2007).

23 Christian, S. D. & Scamehorn, J. F. *Solubilization in surfactant aggregates*. Vol. 55 (CRC Press, 1995).
24 Saville, D. The effects of interfacial tension gradients on the motion of drops and bubbles. *The Chemical Engineering Journal* **5**, 251-259 (1973).
25 Herminghaus, S. *et al.* Interfacial mechanisms in active emulsions. *Soft Matter* **10**, 7008-7022 (2014).
26 Guyon, E., Hulin, J.-P., Petit, L. & Mitescu, C. D. *Physical hydrodynamics*. (Oxford University Press, 2001).
27 Hokmabad, B. V., Saha, S., Canalejo, J. A., Golestanian, R. & Maass, C. C. Quantitative characterization of chemorepulsive alignment-induced interactions in active emulsions. *arXiv preprint arXiv:2012.05170* (2020).
28 Soto, R. & Golestanian, R. Self-assembly of catalytically active colloidal molecules: tailoring activity through surface chemistry. *Physical Review Letters* **112**, 068301 (2014).
29 Hokmabad, B. V., Baldwin, K. A., Krüger, C., Bahr, C. & Maass, C. C. Topological stabilization and dynamics of self-propelling nematic shells. *Physical Review Letters* **123**, 178003 (2019).
30 Cheon, S. I., Batista Capaverde Silva, L., Khair, A. & Zarzar, L. Interfacially-adsorbed particles enhance the self-propulsion of oil droplets in aqueous surfactant. doi:https://doi.org/10.26434/chemrxiv.13426886.v1 (2020).
31 Meredith, C. H. *et al.* Predator–prey interactions between droplets driven by non-reciprocal oil exchange. *Nature Chemistry* **12**, 1136-1142 (2020).
32 Guzowski, J., Korczyk, P. M., Jakiela, S. & Garstecki, P. The structure and stability of multiple micro-droplets. *Soft Matter* **8**, 7269-7278 (2012).
33 Zarzar, L. D. *et al.* Dynamically reconfigurable complex emulsions via tunable interfacial tensions. *Nature* **518**, 520-524, (2015).
34 Carroll, B. J. The kinetics of solubilization of nonpolar oils by nonionic surfactant solutions. *Journal of Colloid and Interface Science* **79**, 126-135 (1981).
35 Gladysz, J. A., Curran, D. P. & Horváth, I. T. *Handbook of fluorous chemistry*. (John Wiley & Sons, 2006).
36 Lippera, K., Benzaquen, M. & Michelin, S. Alignment and scattering of colliding active droplets. *Soft Matter* (2020).
37 Izzet, A. *et al.* Tunable persistent random walk in swimming droplets. *Physical Review X* **10**, 021035 (2020).
38 Paradies, H. H. Shape and size of a nonionic surfactant micelle. Triton X-100 in aqueous solution. *The Journal of Physical Chemistry* **84**, 599-607 (1980).
39 Yu, T. *et al.* Microchannels with Self-Pumping Walls. *ACS Nano*, (2020).
40 Thutupalli, S., Geyer, D., Singh, R., Adhikari, R. & Stone, H. A. Flow-induced phase separation of active particles is controlled by boundary conditions. *Proceedings of the National Academy of Sciences* **115**, 5403-5408 (2018).
41 Krüger, C., Bahr, C., Herminghaus, S. & Maass, C. C. Dimensionality matters in the collective behaviour of active emulsions. *The European Physical Journal E* **39**, 64 (2016).
42 Lach, S., Yoon, S. M. & Grzybowski, B. A. Tactic, reactive, and functional droplets outside of equilibrium. *Chemical Society Reviews* **45**, 4766-4796 (2016).
43 Ross, T. D. *et al.* Controlling organization and forces in active matter through optically defined boundaries. *Nature* **572**, 224-229 (2019).
44 Gentile, K., Somasundar, A., Bhide, A. & Sen, A. Chemically powered synthetic “living” systems. *Chem* **6**, 2174-2185 (2020).